ISSN: 0067-2904

Synthesis of Sodium-Lead Apatite Structure with the Excess and the Lack of Sodium

Mohammed A. B. Abdul Jabar
Department of forensic Science, College of Science, Al-Karkh University of Science, Baghdad, Iraq

Received: 17/4/2022 Accepted: 21/9/2022 Published: 30/5/2023

Abstract

X-ray phase analysis was used to analyse the composition of $Pb_8Na_{(2\pm x)}(PO_4)_6$ (lead-sodium apatite structure) with different X values (X values refer to changes in the excess or lack of sodium (2±X) in the apatite structure): -0.15, -0.10, -0.05, 0.00, +0.05, +0.10, and +0.15. The ceramic method (solid-state reaction) was used to synthesize all samples at a temperature of 800 °C. Many programs, such as match software (v.3), PDF-4 database (ICCD), and database PDF-4 (ASTM), were used to study the single phases. The least-squares method was used to calculate the unit cell parameters. Results have shown that the following compositions: $Pb_8Na_2(PO_4)_6$, $Pb_8Na_{1.95}(PO_4)_6$, $Pb_8Na_{1.90}(PO_4)_6$, and $Pb_8Na_{1.85}(PO_4)_6$ contain only the pure phase of lead sodium apatite structure. On the other hand, the compositions of $Pb_8Na_{2.05}(PO_4)_6$, $Pb_8Na_{2.10}(PO_4)_6$, and $Pb_8Na_{2.15}(PO_4)_6$ showed other phases besides the phases of lead sodium apatite structure.

Keywords: Lead; Apatite; Isomorphic substitutions; Solid solution.

تحضير تركيب صوديوم – رصاص الاباتيت مع زيادة ونقصان في الصوديوم

محمد عبد الباسط عبد الجبار

قسم علوم الادلة الجنائية, كلية العلوم, جامعة الكرخ للعلوم, بغداد, العراق

الخلاصة

تم استخدام طريقة تحليل طور الأشعة السينية لفحص تركيب $Pb_8Na_{(2\pm x)}(PO_4)_6$ (تركيب أباتيت الرصاص–الصوديوم) بقيم X مختلفة (قيم X تعني التغيرات في الفائض أو النقص في كمية الصوديوم (2 ± X) في تركيب الأباتيت): −0.15 ؛ −0.10 ؛ −0.05 ؛ 0.00 ؛ +0.05 ؛ +0.10 و +0.15 لتحديد تأثير فائض ونقص الصوديوم في هذه التركيب. تم اثبات أن طريقة السيراميك (تفاعل الحالة الصلبة) قد حضرت جميع العينات عند درجة حرارة 800 درجة مئوية. تم استخدام العديد من البرامج مثل برنامج Match (الإصدار 3) وقاعدة بيانات PDF−2 (ICCD) وقاعدة البيانات PDF−4 (ASTM) لدراسة الاطوار الفردية. تم استخدام طريقة المربعات الصغرى لحساب معلمات خلية الوحدة. أظهرت النتائج أن التراكيب التالية: $Pb_8Na_2(PO_4)_6$، $Pb_8Na_{1.95}(PO_4)_6$، $Pb_8Na_{1.90}(PO_4)_6$، و $Pb_8Na_{1.85}(PO_4)_6$ تحتوي فقط على الاطوار النقية من تركيب أباتيت الصوديوم. على جانب آخر، اظهرت التراكيب $Pb_8Na_{2.05}(PO_4)_6$،

* Email: mohammed.a.baset1980@gmail.com

$Pb_8Na_{2.10}(PO_4)_6$ و $Pb_8Na_{2.15}(PO_4)_6$ اطوار أخرى إلى جانب اطوار تركيب أباتيت الرصاص – الصوديوم.

1. Introduction

Researchers are interested in chemical materials science and solid-state chemistry due to the problem of isomorphic substitutions since they have used most modern inorganic materials as solid solutions rather than individual compounds. The size of unit cells, interatomic distances, and the distribution of crystallographic positions, the type of chemical bond, and the properties of the crystal structure can all be altered by introducing different additives and varying their amounts [1-3]. Apatite structures are compounds with many properties and could be used in many areas, including industrial, medical, agricultural, environmental, and other fields [4,5]. Isomorphic substitutions are one of the primary features of the crystalline chemistry of apatite compounds because they coexist with several element substitutions in these structures. As is well known, substituting elements within apatite compounds improves crystal formation, which has a significant impact on the physical and chemical characteristics of the compounds [6-8].The existence of two structurally non-equivalent places in the cationic sub-lattice, traditionally termed M (1) and M (2), classifies the apatite structure in the cationic sub-lattice (2). Each M (1) location is surrounded by nine-vertex coordination polyhedrons, which are formed by nine oxygen atoms (each position of PO_4 tetrahedral). Six oxygen atoms form the PO_4 tetrahedron in the coordination environment of the M (2) position, and F^- (Cl^-, OH^-, O^{-2}) ions or vacancy (□) form seven-vertex coordination polyhedrons. In the apatite structure, equilateral triangles M (2) create a conduit where F^- (or Cl^-, OH^-, O^{2-}) ions are inserted. Such compounds' crystal structures belong to the hexagonal system (space group $P6_3/m$) and allow substituting their structural units with other atoms or groups of atoms. The characteristics of the resultant solid solutions can differ greatly from those of the unaltered samples, which broadens the potential applications [9-12]. Lead sodium apatite with the formula $Pb_8A_2(PO_4)_6$, where A = Na, K, Rb, and Cs, is not the last among these compounds. When changed with alkali metals, it becomes a solid electrolyte with cation conductivity. These systems with sodium lead apatite have the advantage that they greatly lower the synthesis temperature to 800 °C when compared to apatites of alkaline earth elements, which streamlines the synthesis process and encourages the formation of excellent grains [13-16]. Many researchers have reported obtaining lead apatites with $Pb_8A_2(GO_4)_6\square_2$ (A = Na, K, Rb, Cs, Tl, Ag; G = P, V, As; □= vacancy), where the conditions of their synthesis and the parameters of unit cells are given. Later, they have been repeatedly investigated by X-ray phase and X-ray diffraction analysis [17-20]. This work aimed to examine the effects of excess and lack of sodium on the lead sodium apatite structure: $Pb_8Na_{(2\pm x)}(PO_4)_6$. The findings can contribute to the development of the isomorphic substitution theory, since lead differs from alkaline earth elements by an ion electron pair that can be activated by isomorphic substitutions.

2. Materials and methods

2.1 Materials

In this research, all samples in the lead sodium apatite structure ($Pb_8Na_{(2\pm x)}(PO_4)_6$) were examined by X-ray solid-phase synthesis with different X values (X values mean the changes in the excess or the lack of sodium (2±X) in the apatite structure): -0.15, -0.10, -0.05, 0.00, +0.05, +0.10 and +0.15. The starting materials (PbO (reagent grade), Na_2CO_3 (reagent grade), and $(NH_4)_2HPO_4$ (analytical grade) were weighed in stoichiometric ratios, mixed in an agate mortar for 20 minutes, and then calcined in alundum crucibles at a temperature of 300 ºC for 3 hours. The temperature was then raised to 800 ºC, where it was calcined for 5-8 hours. Following that, the samples were calcined again at 800 o for 25 hours before being

homogenized. This process was repeated until the phase composition remained constant. As a result, the total calcination time was 40 hours at a temperature of 800 °C.

2.2 Instrumentation

A modernized DRON-3 diffractometer (CuK radiation, Ni filter) was used with electronic control and processing data to perform X-ray phase analysis. During the determination to establish the phase composition of the samples, the counter-rotation speed was 2°/min. [21,22]. We employed the PDF-2 database (ICCD) (International Centre for Diffraction Data) and Match software (v.3) for phase investigation, together with the PDF-4 database (ASTM) (American Society for Testing and Materials) [8,23]. The unit cell characteristics were investigated using the least-squares technique based on 16 individually indexed independent reflections re-scanned at 1° (2θ) / min in the range of $16 \leq 2\theta \leq 54°$. Silicon is utilized as an external standard

.

3. Result and Discussion

For the investigation to observe the effect of excess and lack of sodium on the structure of $Pb_8Na_{(2\pm x)}(PO_4)_6$, samples with different x values (-0.15;-0.10;-0.05;0.00;+0.05;+0.10 and +0.15) were used. Samples were synthesized using the same method as described above. The samples were studied using X-ray diffraction analysis. The results are shown below in Figure 1.

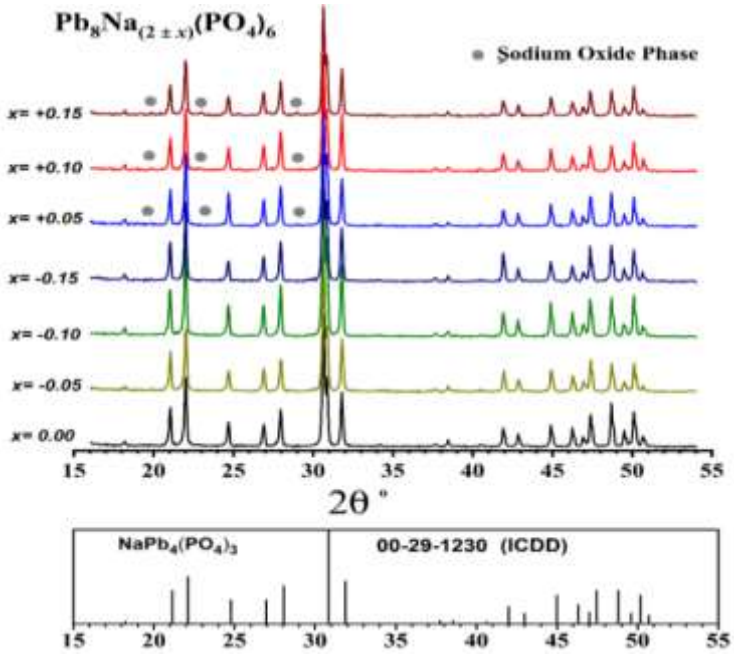

Figure 1: X-ray diffraction patterns of $Pb_8Na_{(2\pm x)}(PO_4)_6$ samples, built according to the pdf-2 database (ICDD).

In the composition of $Pb_8Na_2(PO_4)_6$ and the samples with a lack of sodium: $Pb_8Na_{1.95}(PO_4)_6$, $Pb_8Na_{1.90}(PO_4)_6$, and $Pb_8Na_{1.85}(PO_4)_6$, only reflections of the phase with the lead-sodium apatite structure are found in the X-ray diffraction patterns. Along with reflections of the lead-sodium apatite structure, samples $Pb_8Na_{2.05}(PO_4)_6$, $Pb_8Na_{2.10}(PO_4)_6$, and $Pb_8Na_{2.15}(PO_4)_6$, also contained numerous reflexes that were determined to belong to the sodium oxide phase [7,18]. This is because the intensity of these reflexes of the apatite structure is primarily independent of the value of x, with an intensity of 2-3% compared to Table 1, Figures 2, 3, and 4 show how unit cell characteristics for lead-sodium apatite depend on the composition (a and c).

Table 1: Unit cell parameters of some lead apatites.

Compound	Parameter a, (Å)	Parameter c, (Å)	Reference
$Pb_8Na_2(PO_4)_6$	9.725	7.190	23
$Pb_8Na_2(PO_4)_6$	9.755	7.209	8
$Pb_8Na_2(PO_4)_6$	9.737	7.202	17
$Pb_8Na_2(PO_4)_6$	9.736	7.201	This work

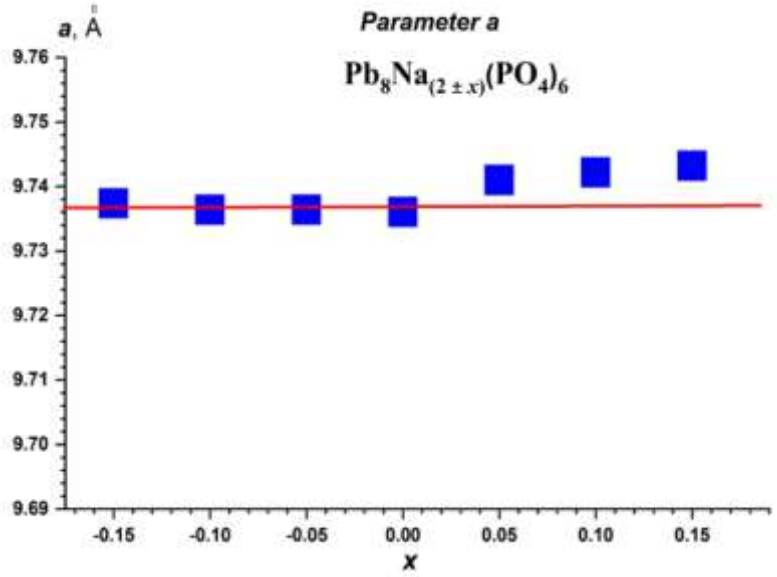

Figure 2: Dependence of the unit cell parameter (a) of the apatite structure in the $Pb_8Na_{(2\pm x)}(PO_4)_6$ system *vs*. the composition (x).

As can be seen from the data, we noticed that the parameters of the samples with excess sodium increased slightly (the inaccuracy of the parameters lies within ±0.003 Å) due to the immiscibility of the excess sodium present with the components of the pure lead apatite compound and led to the emergence of a new phase (NaO phase). In addition to the sodium apatite phase, the parameters were thus increased. No change in the parameters was impacted by the decrease in sodium in the pure lead apatite compound [23, 24].

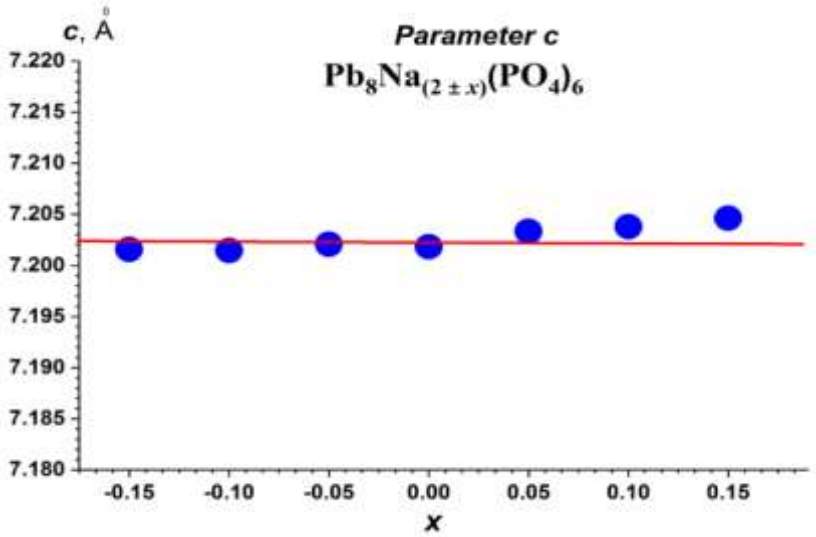

Figure 2: Dependence of the unit cell parameter (c) of the apatite structure in the $Pb_8Na_{(2\pm x)}(PO_4)_6$ system *vs*. the composition (x).

4. Conclusion

The solid-phase synthesis technique was used to examine the synthesis of samples of the lead-sodium apatite structure with the formula $Pb_8Na_{(2\pm x)}(PO_4)_6$ at a temperature of 800 ºC to determine the effect of excess and lack of sodium in this structure [25,26]. The samples with x values of -0.15, -0.10, -0.05, and 0.00 contain only a pure phase of lead sodium apatite structure, as shown by the unit cell features (a and c) and the outcomes of the X-ray diffraction data analysis. While in the samples with x values of +0.05, +0.10, and +0.15, another solid phase (sodium oxide) besides the pure phase of lead sodium apatite was found, it can be assumed this is a super-structural reflex, or a reflex of a component that does not enter the structure isomorphically, or the sodium excess in the systems reacts with oxygen to form sodium oxide [27,28].

Acknowledgements

We appreciate all the people who supported our work or helped us prepare, measure, and analyse all the samples in this manuscript.

Conflict of Interests

The author declare that they have no conflicts of interest to this article.

References

[1] E. I. Get'man, Y. A. Oleksii, S. V. Radio, and L. I. Ardanova, "Determining the phase stability of luminescent materials based on the solid solutions of oxyorthosilicates $(Lu_{1-x}Ln_x)$ $[(SiO_4)_{0.5}O_{0.5}]$, where Ln = La-Yb," *Fine Chemical Technologies*, vol. 15, no. 5, pp. 54-62, 2020.

[2] L. I. Ardanova, E. I. Get'man, S. V. Radio, I. M. Hill, and A. V. Ignatov, "Isomorphous Substitutions in Luminescent Materials Based on $ScVO_4$," *Key Engineering Materials*, vol. 865, pp. 37-42, 2020.

[3] L. I. Ardanova, K. Chebyshev, A. V. Ignatov, L. Pasechnik, N. Selikova, E. I. Get'man, and S. Radio, "Fluorite-Like Neodymium Molybdates Doped with Lead," *Key Engineering Materials*, vol. 865, pp. 49-53, 2020.

[4] P. Ptáček, *Apatites and their Synthetic Analogues - Synthesis, Structure, Properties and Applications*, published by IntechOpen, 2016, p. 516.

[5] A. R. West, *Solid State Chemistry and its Applications*, 2nd ed., John Wiley and Sons, 2014, p. 584.

[6] L. E. Smart, *Solid State Chemistry: An Introduction*, 4th Ed., CRC Press, 2012, p. 442.

[7] J. D. Hopwood, G. R. Derrick, D. R. Brown, C. D. Neman, J. Haley, R. Kershaw, and M. Collinge, "The Identification and Synthesis of Lead Apatite Minerals Formed in Lead Water Pipes," *Journal of Chemistry*, vol. 2016, pp. 1-11, 2016.

[8] M. A. B. Abdul Jabar, "Studying Solid Solutions of Substitution of Pb with Sm in Lead-Sodium Apatite Structure," *Nanosistemi, Nanomateriali, Nanotehnologii*, vol. 17, no. 2, pp. 334-352, 2019.

[9] M. A. B. Abdul Jabar and A.V. Ignatov, "New Synthesis of Solid Solution lead hydroxyapatite (PbHAP) by Ceramic and Semi-Ceramic Methods," *Journal of the Chemical Society of Pakistan*, vol. 42, no. 3, pp. 363-368, 2020.

[10] N. Tram, K. Ishikawa, T. Minh, D. Benson, and K. Tsuru, "Characterization of carbonate apatite derived from chicken bone and its in-vitro evaluation using MC3T3-E1 cells," *Materials Research Express*, vol. 8, no. 2, pp. 1-11, 2021.

[11] L. K. Tran, K. R. Stepien, M. M. Bollmeyer, and C. H. Yoder, "Substitution of sulfate in apatite," *American Mineralogist*, vol. 102, no. 10, pp. 1971-1976, 2017.

[12] M. Maruuta, T. Arahira, K. Tsuru, and S. Matsuya, "Characterization and thermal decomposition of synthetic carbonate apatite powders prepared using different alkali metal salts," *Dental Materials Journal*, vol. 38, no. 5, pp. 750-755, 2019.

[13] Y. Zhou, C. Liao, K. Shih, G. Tan, and M. Su, "Incorporation of lead into pyromorphite: Effect of anion replacement on lead stabilization," *Waste Management*, vol. 143, pp. 232-241, 2022.

[14] Y. Foucaud, I. V. Filippova, and L. O. Filippov, "Investigation of the depressants involved in the selective flotation of scheelite from apatite, fluorite, and calcium silicates: Focus on the sodium silicate/sodium carbonate system," *Powder Technology*, vol. 352, pp. 501-512, 2019.

[15] Z. Pan, Y. Wang, Q. Wei, X. Chen, F. Jiao, and W. Qin, "Effect of sodium pyrophosphate on the flotation separation of calcite from apatite," *Separation and Purification Technology*, vol. 242, pp. 1-19, 2020.

[16] C. Ibsen, H. Leemreize, B. Mikladal, J. Skovgaard, M. Bremholm, J. Eltzholtz, B. Iversen, and H. Birkedal, "Alkali Counterions Impact Crystallization Kinetics of Apatite Nanocrystals from Amorphous Calcium Phosphate in Water at High pH," *Crystal Growth & Design*, vol. 18, no. 11, pp. 6723-6728, 2018.

[17] M. A. B. Abdul Jabar, E. I. Getman, and A. V. Ignatov, "New gadolinium-substituted lead sodium apatite structure," *Functional Material*, vol. 25, no. 4, pp. 713-719, 2018.

[18] L. Pajchel, and L. Borkowski, "Solid-State NMR and Raman Spectroscopic Investigation of Fluoride-Substituted Apatites Obtained in Various Thermal Conditions," *Journal ofMaterials*, vol. 14, no. 22, pp. 1-13, 2021.

[19] Y. Zhu, B. Huang, Z. Zhu, H. Liu, Y. Huang, X. Zhao, and M. Liang, "Characterization, dissolution and solubility of the hydroxypyromorphite–hydroxyapatite solid solution $[(Pb_xCa_{1-x})_5(PO_4)_3OH]$ at 25 °C and pH 2-9," *Geochemical Transactions*, vol. 17, no. 2, pp. 1-18, 2016.

[20] I. Grynyuk, O. Vasyliuk, S. Prylutska, N. Strutynska, O. Livitska, and M. Slobodyanik, "Influence of nanoscale-modified apatite-type calcium phosphates on the biofilm formation by pathogenic microorganisms," *Open Chemistry Journal*, vol. 19, pp. 39-48, 2021.

[21] S. Iconaru, M. Motelica-Heino, R. Guegan, M. Beuran, A. Costescu, and D. Predoi, "Adsorption of Pb (II) Ions onto Hydroxyapatite Nanopowders in Aqueous Solutions," *Journal of Materials*, vol. 11, no. 11, pp. 1-17, 2018.

[22] M. Baaziza, M. Azdouz, M. Azrour, A. Batan, and B. Manoun, "Elaboration, Rietveld refinements and vibrational spectroscopic studies of a new lacunar apatite series: $NaPb_{3-x}Ca_xCd(PO_4)_3$ $(0\leq x\leq 1)$," *Journal of Chemical Research*, vol. 42, pp. 564-571, 2018.

[23] L. El Koumiri, S. Oishi, S. Sato, L. El ammari, and B. Elouadi, "The crystal structure of the lacunar apatite $NaPb_4(PO_4)_3$," *Materials Research Bulletin*, vol. 35, pp. 503-513, 2000.

[24] L. Denisova, M. Molokeev, A. Aleksandrovskii, Yu. Kargin, E. Golubeva, and V. Denisov, "Crystal Structure, Luminescence, and Thermodynamic Properties of $Pb_{10-x}Eu_x(GeO_4)_{2+x}(VO_4)_{4-x}$ (x= 0.1, 0.2, 0.3) Substituted Apatites," *Inorganic Materials*, vol. 57, pp. 1158-1166, 2021.

[25] H. A. AlMashhadani and K. A. Saleh, "Electrochemical Deposition of Hydroxyapatite Co-Substituted By Sr/Mg Coating on Ti-6Al-4V ELI Dental Alloy Post-MAO as Anti-Corrosion," *Iraqi Journal of Science*, vol. 61, no. 11, pp. 2751-2761, 2020.

[26] N. A. Al-eesa, A. Johal, R. G. Hill, and F. S. L. Wong, "Fluoride containing bioactive glass composite for orthodontic adhesives - Apatite formation properties," *Dental materials*, vol. 34, no. 8, pp. 1127-1133, 2018.

[27] K. S. Al-Bassam, "A Reconnaissance Study of Rare Earth Elements Systematic in Phosphate Coprolites: Comparison between Continental Shelf and Intracontinental Basin Deposits," *Iraqi Journal of Science*, vol. 63, no. 6, pp. 2566-2581, 2022.

[28] C. Zhou, X. Wang, X. Song, Y. Wang, D. Fang, S. Ge, and R. Zhang, "Insights into dynamic adsorption of lead by nano-hydroxyapatite prepared with two-stage ultrasound," *Chemosphere*, vol. 253, pp. 1-11, 2020.